RESEARCH ARTICLE

WILEY

# Non-destructive techniques for structural characterization of cultural heritage: A pilot case study

**Eleonora Spoldi** ⬤ | **Ileana Ippolito** ⬤ | **Alberto Stella** ⬤ | **Salvatore Russo**

Dipartimento di Culture del Progetto, Università Iuav di Venezia, Venice, Italy

**Correspondence**
Eleonora Spoldi, Dipartimento di Culture del Progetto, Università Iuav di Venezia, Dorsoduro 2206, 30123, Venice, Italy.
Email: espoldi@iuav.it

**Summary**

This work describes an approach for combining local and global non-destructive techniques for the structural characterization and conservation assessment of cultural heritage buildings. An experimental investigation program was conducted on the south vault of St. Mark's Basilica in Venice, involving historical investigations, a damage survey, sonic tests, and ambient vibration measurements. Recorded data were employed to assess the material and structural properties of the vault and to characterize the observed damage pattern. The study of the correlation between results of sonic tests and ambient vibration measurements has shown how, in complex structural typologies, the information provided by both these two kinds of tests are necessary in order to effectively characterize the structural behaviour, which is strongly influenced by the complexity of geometry and restraint condition. Experimental results have been used for the validation of a numerical model adopting a non-conventional approach. The procedure is based on comparing numerical simulation of ambient vibration response in terms of the frequency content of acceleration signals. This approach can be performed using only a limited number of measured acceleration signals, proving to be useful and cost-effective. The work aims to provide helpful insights into the combined use of non-destructive tests for the efficient structural characterization and safety assessment of heritage structures.

**KEYWORDS**
ambient vibration analysis, ND tests, sonic tests, St. Mark's Basilica in Venice, vibration measurement

## 1 | INTRODUCTION

Cultural heritage and historical buildings are present in almost every country and have a fundamental social and economic impact. However, material ageing processes and various natural risks can significantly affect their architectural and structural conditions. The safety assessment of these constructions is a complex task since little information are usually available regarding their structural behaviour. Variability of mechanical properties through the structure, existing damages and deterioration phenomena, and lack of knowledge on the constitution of the inner core of the elements are among the significant problems encountered.[1,2] Moreover, each cultural heritage building is unique and often during its lifetime it has experienced several structural and non-structural changes, which can have strongly affected its load-carrying capacity.[3]

The preservation of cultural heritage buildings experienced a significant improvement in the last two decades, due to the development of operational techniques for the analysis and problem diagnosis of these particular structures.[4] A general preservation procedure can be subdivided into three main stages, namely, *diagnosis*, concerning the assessment of the structural reliability; *prognosis*, defining possible restoration works; *prediction* of the temporal evolution of the structural behaviour based on tests and monitoring data.[5]

In addition to the three preceding stages, some preliminary and complementary activities have to be done. The first is the historical investigation about the major restoration and modification works that took place during the structure lifetime, which helps detecting degradation phenomena and the works that have been done to get rid of them. The following step concerns the monument detailed geometrical description, which represents a quite difficult task since the architectural shapes are often very complex and highly variable. The third step is related to the investigations necessary to achieve adequate knowledge about mechanical properties of the materials. This aim can be achieved through a convenient set of experimental tests carried out on relevant structural elements, and it is particularly important in the case of rehabilitation of a historical building. In many cases, a monitoring period is needed in order to investigate the structural behaviour as a function of time and of environmental conditions changes.[6,7]

Nowadays, non-destructive (ND) tests are of fundamental importance in structural health monitoring (SHM) practices, since they can provide valuable information about material and structural properties[8] without the difficulties and time consumption related to destructive tests. In addition, analysis of recorded ambient vibrations provides additional insights into the global structural behaviour,[9,10] especially by optimizing the type and configurations of sensors.[11]

This work presents a study on the combined use of local and global ND techniques for the structural characterization of highly complex structures, using the results of a ND diagnostic campaign performed on a historical damaged masonry vault. The case study investigated is the south vault of the St. Mark's Basilica in Venice, Italy. An experimental campaign has been carried out on the vault, performing sonic tests and ambient vibration measurements in order to evaluate the dynamic elastic modulus of masonry and the dynamic behaviour of the vault. Moreover, sonic tests were employed to evaluate the depth of the two main cracks and to study the adhesion between mosaics and masonry.

The primary aim of this work is to provide insights into the structural behaviour of the vault, which is currently characterized by large cracks which compromise not only its structural integrity but also the condition of mosaics placed on the inner surface of the vault.

Experimental results have been employed to test a numerical calibration procedure based on ambient vibration simulation, in which the frequency content of experimental acceleration histories has been compared with its numerical counterpart obtained from numerical time-history simulations.

A similar approach, employing the numerical simulation of the ambient vibration response, was presented by Pepe et al.,[12] with the aim of implement and numerically monitor the effects of progressive damage developing in a structure.

Several works presented approaches for the structural modelling of the St. Mark's Basilica. The work of Rossi[13] presented a numerical model developed using results from a photogrammetric survey of the entire basilica, carried out during a diagnostic campaign conducted by ISMES (Bergamo, Italy) in the early 90s. The experimental campaign also allowed to evaluate the mechanical characteristics of the materials. The model represents the whole geometry of the basilica and also a portion of the foundation soil. In order to deal with the model complexity, five substructures were identified, each one containing a dome and its underlying supporting structure. The numerical response of the basilica for gravity loads and seismic actions has been presented, respectively, by Mola and Vitaliani[5] and Oñate et al.[14] These studies highlighted that detailed geometric description of interface zones and advanced non-linear material modelling are necessary to reproduce the structural behaviour of the global structure subjected to both gravity and dynamic loads.

In the present study, two numerical models were developed. The first represents only the vault, while the other also includes part of the vault supporting structures. Both models are simplified representations, since they represent only a small portion of the global structure of the basilica. The numerical response of the structure to ambient vibration was simulated through linear time–history analyses, whose results have been compared with acceleration data recorded on the vault. Ambient vibrations were simulated as both artificial and recorded acceleration histories applied at the matroneum floor. The comparison allows checking both the models capabilities and limitations in reproducing the structural behaviour of the vault and provides useful information for future model updating. Performed experimental tests provided both material properties data and vibration measurements for model calibration. Data recorded using the tromograph device have demonstrated to be comparable with the numerical response, so they can be effectively used in a model calibration procedure.

## 2 | DESCRIPTION OF THE CASE STUDY

St. Mark's Basilica is an extraordinary cultural heritage for several reasons. Apart from the artistic value of its architecture and pieces of art, the most outstanding characteristic is its lively complexity. In St. Mark's Basilica, a continuous restoration process is currently ongoing, aiming to the conservation of structures, mosaics, and several details, performed by many experts who work full time. In this context, knowledge of the architecture of the basilica and its state of preservation appears to be very relevant, as it represents a guide for interventions and management of the whole complex.[15] The basilica was built over a time spanning many centuries, using the previously existing structures as possible. Nowadays, it shows clear signs of deformation and degradation of many architectural and structural elements, including walls, arches, vaults, domes, and floors. Several earthquakes have contributed to worsening the static conditions of the basilica, particularly in the 12th century. Moreover, many devastating fires occurred, which made necessary the reconstruction of entire parts of the structure. During its lifetime, the basilica has undergone several changes, such as the weightening of the domes and the installation of additional elements to the load-bearing structures.[16]

The St. Mark's Basilica has a floor plan in the shape of a Greek cross (Figure 1), with a dome over the crossing and another dome on each of the four arms. The nave and the transept have a central aisle and two side aisles divided by an arcade. The nave of the upper arm, corresponding to the presbytery, is raised by a few steps, below whom is located the crypt. To the sides of the presbytery, there are two chapels. The presbytery area is separated from the rest of the basilica by the iconostasis, which is divided into three distinct sections: the central one, in front of the presbytery, and the two lateral parts, in front of the chapels. The upper inner perimeter of the entire basilica, except for the apse, is crossed by the matroneum. A narthex wrapped around the west end disguises the cross shape but creates a wide surface for the main facade. The church architectural structure and its ornaments are byzantine; however, Gothic and Romanesque styles can also be found in the decorations. Marble slabs, sculpture, and golden mosaics completely hide the church main brick structure, both inside and outside.

The diagnostic analyses illustrated by Rossi[13] represent an exhaustive example of the methodological approach that should be followed when studying the static behaviour of an important monument. Such a combined experimental and numerical procedure is actually an effective tool for the study and design of restoration and consolidation works. In particular, the results of the experiments have been used to evaluate the composition, strength, and stiffness of the masonry, as required to develop the numerical model.

The vault analysed in the present work is located at the south end of the transept (Figure 1). It is one of four connecting vaults located under the south dome. The vault is bordered on the short sides by massive masonry pillars, while on the side facing outwards, it consists of masonry and a large rose window (Figure 2). The side facing the nave has a large arch supporting the dome above.
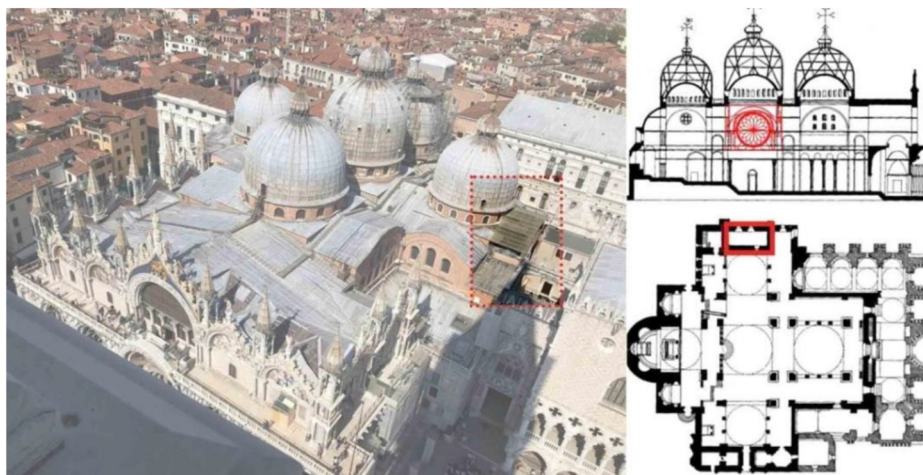


**FIGURE 1** Global view and vertical and horizontal sections of the St. Mark's Basilica. In the red rectangle, the location of the south vault is indicated
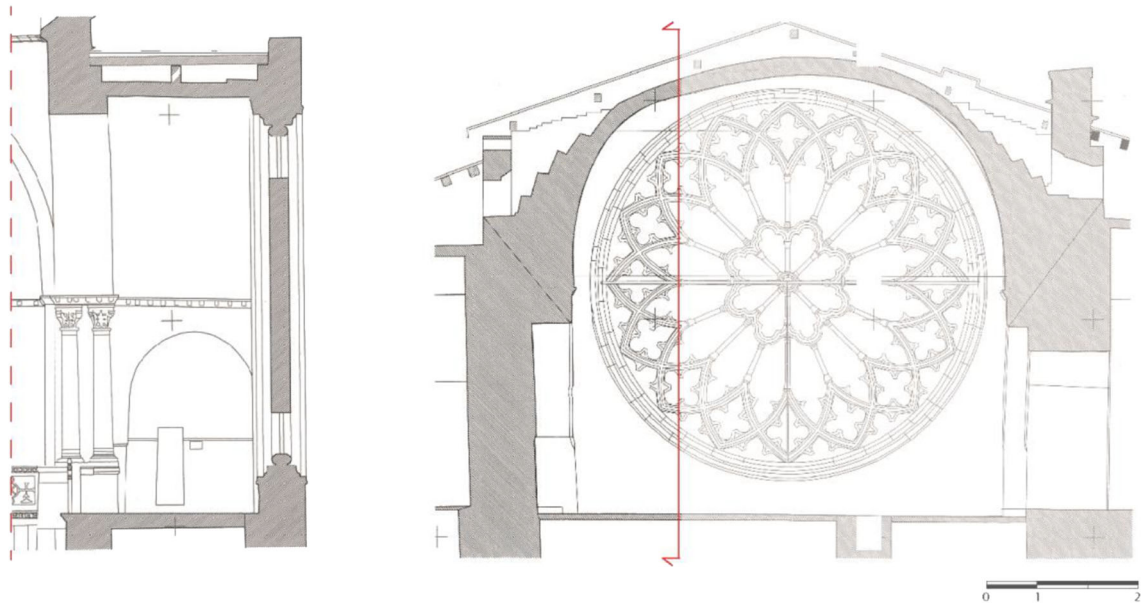
**FIGURE 2** Transverse and longitudinal sections of the studied vault
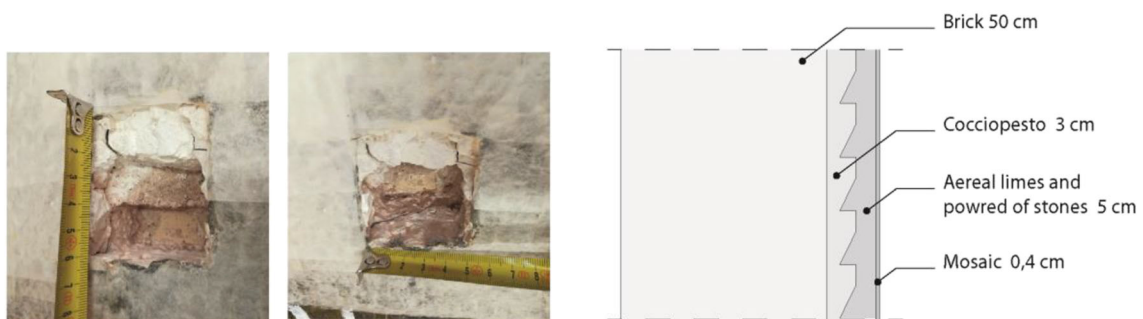


**FIGURE 3** Masonry stratigraphy

The vault intrados is covered with mosaic tiles made in various historical periods: the central mosaics of the vault are from 1400, those along the lateral parts of the vault were made around 1670 and those around the rose window date back to 1850.

A previously performed survey provided the stratigraphy of the walls supporting the vault. They are composed of, starting from the inside, a 0.4-cm mosaic, a 5-cm aerial lime and stone power layer, a 3-cm *cocciopesto* layer, and a 50-cm load-bearing masonry wall (Figure 3).

Plans of the structure reported that the vault is curved along one direction only, but the curvature is not constant. The western portion is lower than the eastern one, as shown in Figure 2. A visual in situ inspection of the vault showed that the vault extrados presents a series of diagonal cracks along the mortar joints, as visible in Figure 4, while the vault intrados shows a diagonal crack extending to about one-third of its entire development. The outer and inner major cracks are not coincident. The vault inner surface has been secured by positioning sheets that cover the mosaics and a series of wooden ribs to avoid inner layers collapse.

# 3 | EXPERIMENTAL CAMPAIGN

A non-destructive experimental diagnostic campaign was carried out on the south vault of St. Mark's Basilica. The main purposes of the study include the assessment of the damage level of the structure, the determination of the main mechanical properties of masonry, and the experimental evaluation of the vibration frequencies of the vault.[17]
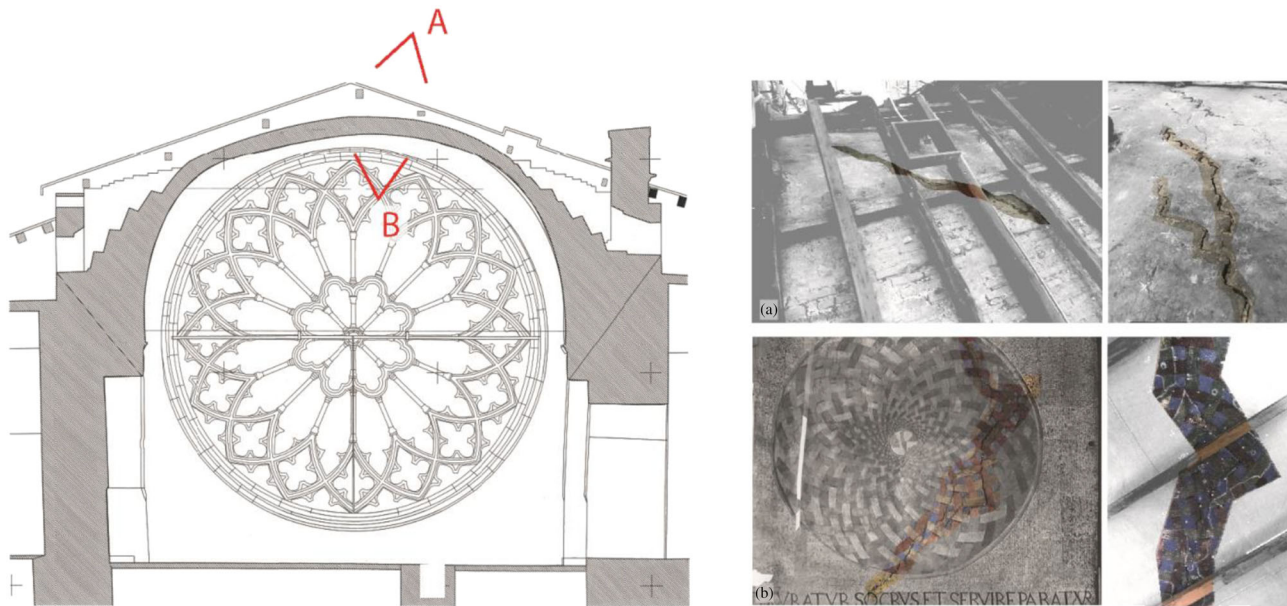
**FIGURE 4** View of the cracks at the extrados (a) and intrados (b) of the vault



(a)　　　　　　　　　　　　　(b)

**FIGURE 5** In situ measurements using (a) sonic testing and (b) tromograph device

Two kinds of measurements have been conducted: sonic tests (Figure 5a) and microtremors measurements (Figure 5b). The sonic investigation technique is based on the principle that the propagation velocity of elastic waves in a solid is related to the material mechanical and physical characteristics. This technique is based on elastic waves in the sound frequency range (20 Hz–20 kHz), generated by a mechanical impulse applied to the structure. In particular, the propagation velocity of a wave moving through an elastic, homogeneous, and isotropic solid is a function of the dynamic elastic modulus, the Poisson coefficient, and the solid density.

In masonry elements, due to the intrinsic heterogeneity and anisotropy and to the variability of existing typologies, the sonic wave velocity cannot be directly related to the solid properties. However, previous works have shown that, for a specific masonry, a marked relationship can be identified between the velocity values of the sonic waves and the modulus of elasticity of the masonry.[18] Furthermore, it has been widely demonstrated that sonic tests can be correctly used to conduct local analyses and to obtain qualitative information on the consistency of the masonry.[19,20]

For the microtremor measurements, a Tromino® device has been used.[21] This device optimizes the microtremor measurement in the frequency range between 0.1 Hz and 200 Hz using output-only measurements. The device is equipped with several transducers: three high-resolution electrodynamic velocimeter channels to acquire the environmental microtremor up to approximately ±1.5 mm/s; three velocimetric channels for recording strong vibrations up to ±5 cm/s; and three accelerometric channels. The sensors measure along three directions and transmit the signal to a

digital acquisition system. Recorded data are then processed using the software Grilla® [22] and Matlab.[23] Further details on the operating principle of the adopted instrumentation and methodology can be found in Russo and Spoldi.[24]

Sonic tests were carried out to qualitatively characterize the extent of the damage on the vault. First of all, the depth of the cracks at the extrados and intrados was investigated. Then, a second analysis involved the study of the adhesion between the mosaics and the supporting structure to identify the most vulnerable points of the decorative apparatus.

The experimental measure of a superficial crack depth is often difficult and can be affected by uncertainties, since cracks are usually not perfectly orthogonal to the surfaces where measures are taken. In order to overcome this problem, a sufficiently large data population has been obtained by selecting 80 measurement points to perform the test, as shown in (Figure 6a). The distance between the measurement points identified with capital letters is about 20 cm, while the distance of those identified by the numbers 1 to 4 is 16 cm (Figure 6a). The test was repeated twice, adopting two configurations. In the first one, the hammer hit the position 2, while the accelerometers were placed at positions 1 and 3. In the second configuration, the hammer hit the position 3, and the accelerometers were placed at positions 2 and 4. The experimental measurements revealed a depth of the intrados crack between 6 and 18 cm with an average depth of 12.5 cm. Among the measurements made, it was chosen to exclude the L measurements because they have values discordant with the average of the data, possibly due to the crack bifurcation, which could have influenced the propagation time measurement.

The same experimental technique for estimating the crack depth has also been applied to the crack present on the extrados of the vault. However, due to site-related difficulties in positioning sensors on the extrados, the number of measurement points has been reduced. For the extrados, 48 measurement points were chosen (Figure 6b). Recorded data revealed a depth of the extrados crack between 7 and 15 cm with an average depth of 10.5 cm.

The performed tests showed that the cracks are partially overlapped. Along the overlapping zone, 1/3 of the vault thickness is affected by the damage and consequent loss of stiffness of the structure is expected.

The entire development of the vault intrados has been also involved in *indirect* sonic tests for the assessment of mosaic adhesion conditions. Sonic measurements revealed differences in propagation velocity values between the undamaged zone and the cracked vault portion.

The arrangement of the measurement points involved in the tests is shown in Figure 7. A total of 168 measurements were taken, placing the sensors along two orthogonal directions, that is, perpendicular and parallel to the vault axis.
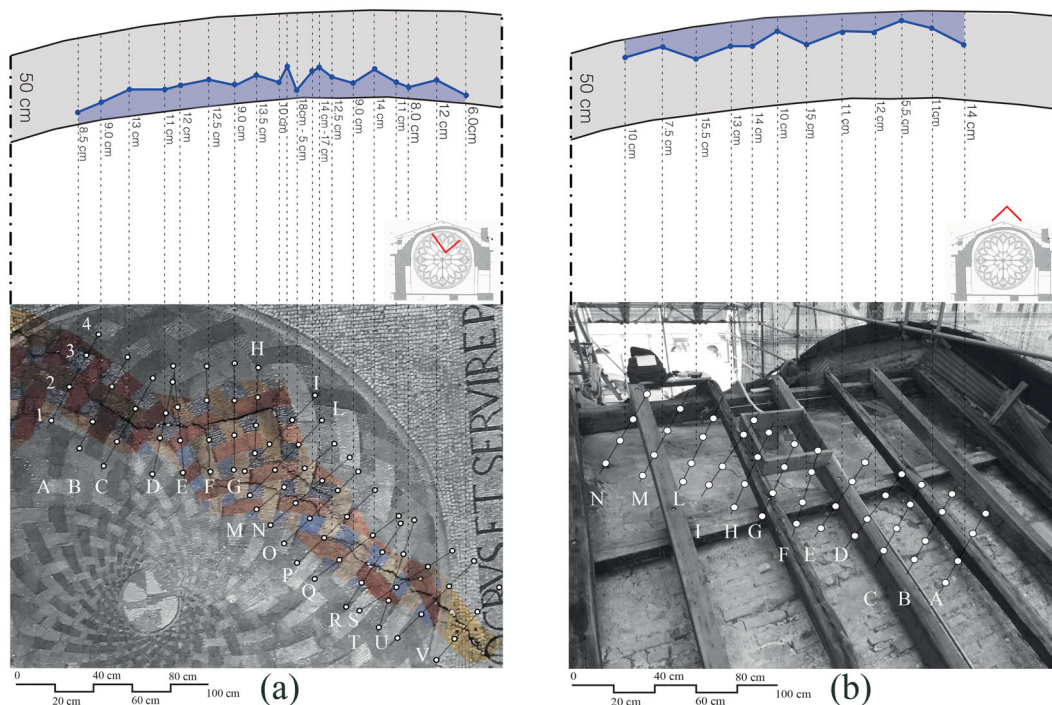


**FIGURE 6** Damage survey and experimental measurement of crack depth: (a) Crack at the vault intrados; (b) crack at the vault extrados
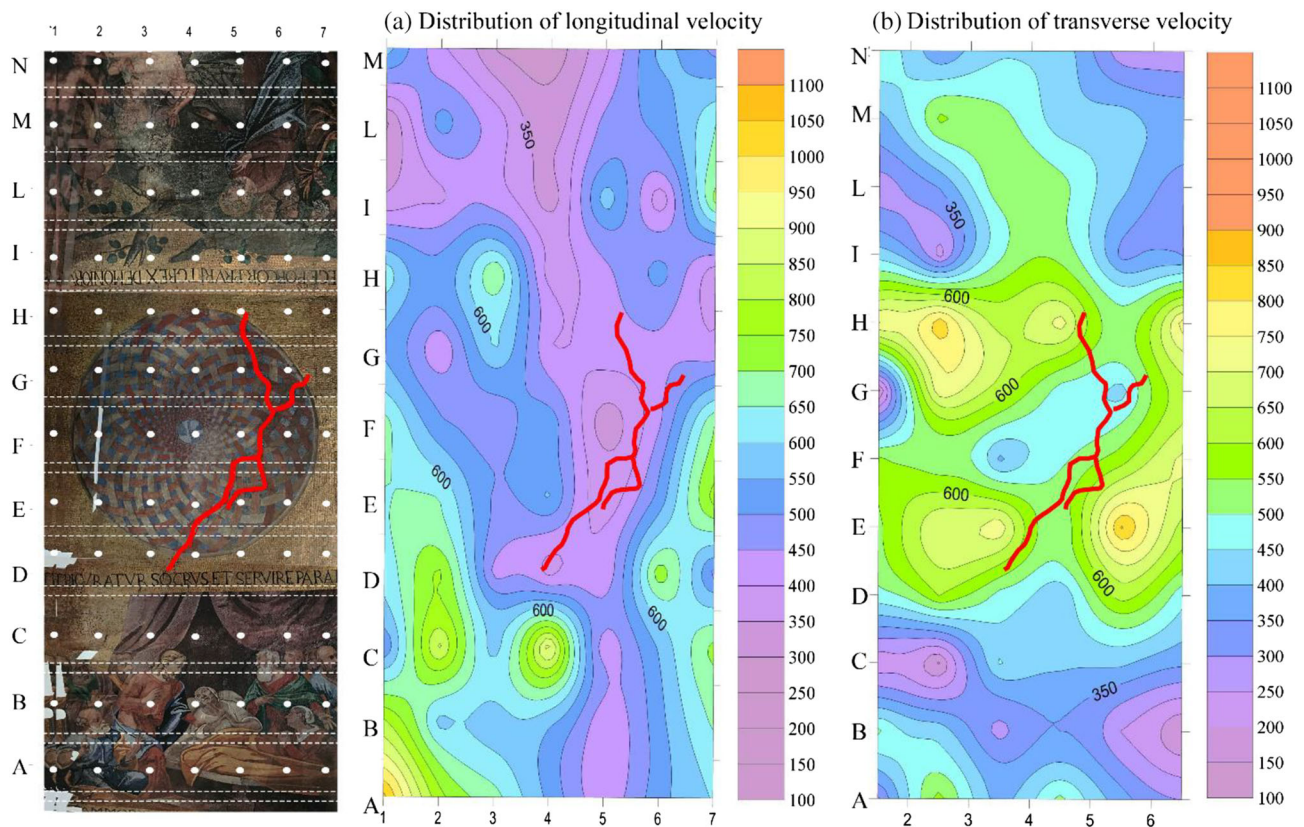
**FIGURE 7** Distributions of propagation velocity obtained from indirect sonic tests conducted on the vault intrados

For measuring in-plane propagation velocity on the vault, sensors have been positioned in sectors delimited by the same ribs. For measures of propagation velocity along the longitudinal direction, the tests were performed so as, for example, if the hammer hit the position A1, the accelerometers were placed at positions A2, A3, A4, A5, and A6, indicated in Figure 7. The average propagation velocity along the longitudinal direction obtained by the indirect sonic tests is 467 m/s, with a standard deviation of ±162 m/s (Figure 7a).

Conversely, for measurement of propagation velocity along the transverse direction, the sensors have been positioned so as, for example, if the hammer hit the position A1, the accelerometers were placed at positions B1 and C1, indicated in Figure 7. The average propagation velocity in the transverse direction obtained from the indirect sonic test is 524 m/s with a standard deviation of ±160 m/s (Figure 7b).

In the central portion of the vault, the average propagation velocity was equal to 523 m/s along the longitudinal direction and equal to 543 m/s along the transverse direction. For the eastern portion of the vault, an average propagation velocity of 467 m/s and 400 m/s was found for the longitudinal and transverse directions, respectively. The most significant differences in the results along the two orthogonal directions involve the western portion of the vault, which presents propagation velocity values of 632 m/s and 365 m/s for the longitudinal and transverse directions, respectively.

Despite this, in Figure 7a,b, it can be noted how, for both directions, the presence of the crack strongly reduces the propagation velocity of the sonic waves, highlighting low characteristics of adherence and homogeneity between the substrate and the load-bearing structure in lines E to H.

*Direct* sonic tests were carried out for the qualitative evaluation of the masonry compactness of the vault. These measurements involved the zones around the cracks visible both on the vault intrados and extrados.

Figure 8 illustrates the distribution of propagation velocity along the direction orthogonal to the vault surface. The average velocity is 784 m/s, with a standard deviation of ±240 m/s.

For direct sonic tests, as observed for indirect ones, analysis of velocity distribution shows how the presence of the cracks decreases the sonic waves velocity. In Figure 8, the profile of the crack is clearly recognizable in columns 4 to 6. In these columns, the average propagation velocity is about 650 m/s, which is much lower than the overall average velocity, equal to 874 m/s.
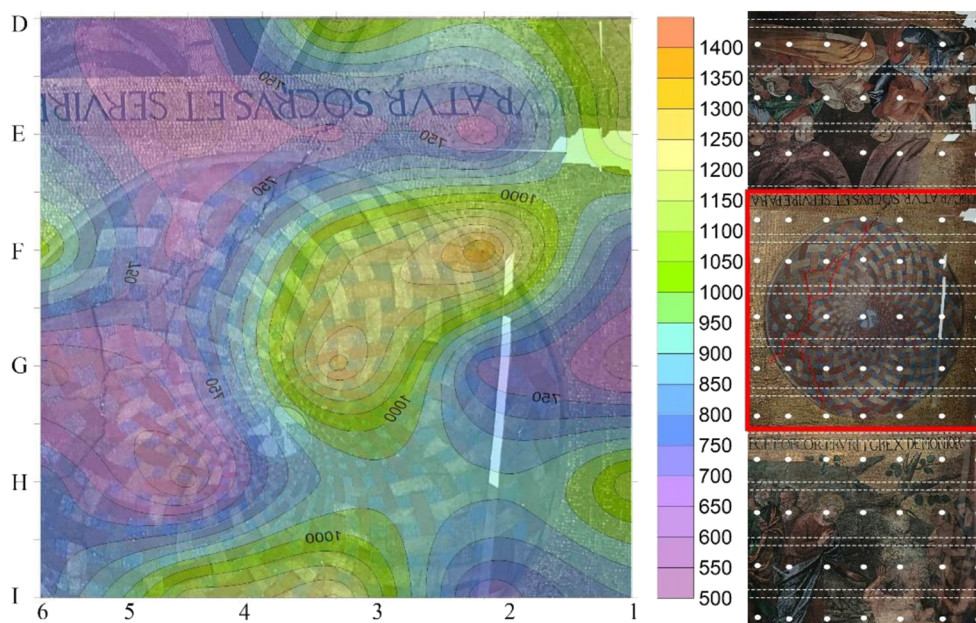
**FIGURE 8** Distribution of propagation velocity obtained from direct sonic tests for the central portion of the vault
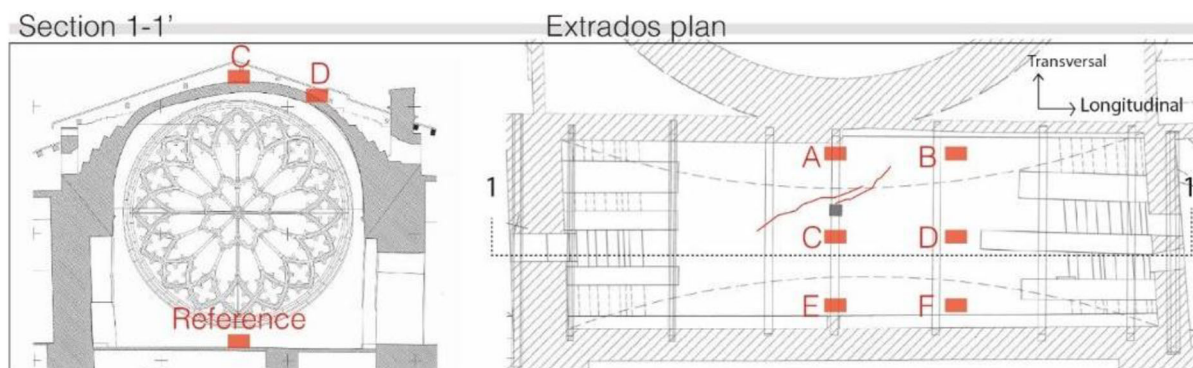


**FIGURE 9** Locations at which ambient vibrations were recorded

The latter value was used to calculate the average experimental dynamic elastic modulus, equal to 3143 MPa. The elastic modulus value for the cracked portion of the vault is 1740 MPa, while the average elastic modulus for the non-cracked portion of the vault is 3150 MPa.

An estimation of the elastic modulus was also performed for the north-western support of the vault, using *indirect* sonic tests. The obtained average elastic modulus is equal to 4039 MPa, corresponding to a recorded average propagation velocity of 991 m/s. These results agree with the ones obtained from the surveys carried out in the basilica by the ISMES,[13] which identified an elastic modulus between 800 and 2000 MPa for old or cracked masonry and between 1600 and 4000 MPa for consolidated masonry.

A series of ambient vibration measurements were performed on selected measurement points at the matroneum level and on the vault outer surface. In particular, six measurement points (A to F) were selected on the extrados and one on the matroneum (Reference). The locations of the measurement points are shown in Figure 9.

Velocity and acceleration were sampled at 512 Hz for a time interval of 16 min. The time histories were analysed by breaking the signal into 20-s windows and using a triangular window filter with 5% smoothing. Fast Fourier transformation (FFT) of recorded signals was performed, and spectra were analysed in the frequency range 0–64 Hz since the lower natural frequencies of the masonry structure are expected to belong to this range. It was observed that major amplitudes are concentrated in the frequency range between 5 Hz and 30 Hz. In Figure 10, FFTs of the acceleration
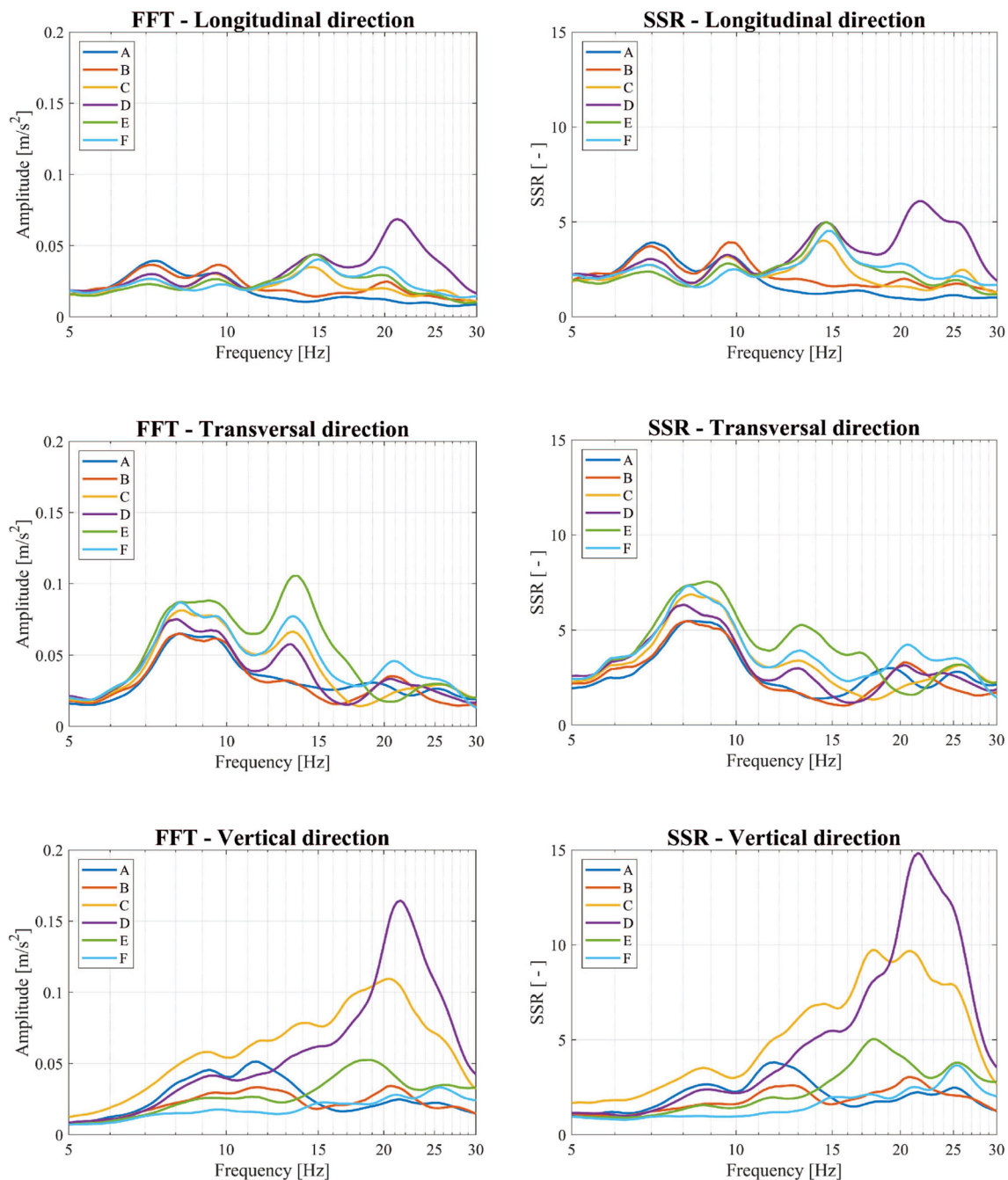
**FIGURE 10** FFTs and SSRs of acceleration signals recorded on the vault. SSRs were evaluated using the spectra of signals measured at matroneum as reference

signals recorded on the vault are presented, for components related to longitudinal, transversal and vertical directions, where the transversal direction is orthogonal to the rose window.

Spectral acceleration amplitudes were used to calculate the spectral standard ratio (SSR) for the measurement points of the vault. The SSR is calculated as a ratio between spectral values related to homologous components. In this case, the ratio's numerator is represented by a spectral ordinate related to a measurement point of the vault, while the denominator—also called reference measure—is represented by the corresponding spectral ordinate obtained for the measurement point on the matroneum. Performing SSR, part of the reference signal ambient noise can be subtracted from the target signals related to the vault extrados. In this way, by analysing SSR, the vault main vibration frequencies can be clearly identified.

In Figure 10, SSRs of the acceleration signals recorded at the vault are also presented. Although spectra are not characterized by well-defined and isolated peaks, particularly high amplitudes are identified at specific frequency ranges, especially for the transverse and vertical components. In all signals, the transverse component is accentuated in a frequency range between 8 and 10 Hz, with a lower amplitude peak present in the range 12–14 Hz. Peaks also related to the longitudinal component can observed in the latter range, while high-amplitude peaks for the vertical component can be observed in the range 20–22 Hz.

According to the observations mentioned above, the first vibration mode of the vault is identified in the range 8–10 Hz, having a modal shape that moves along the transverse direction. A second vibration mode is identified in the frequency range between 13 and 14 Hz in which part of the vault surface moves along the longitudinal direction. The third identified vibration mode is associated with a frequency belonging to the range 20–22 Hz and is related to the vibration of the vault along the vertical direction.

# 4 | NUMERICAL MODAL ANALYSIS AND AMBIENT VIBRATION RESPONSE SIMULATION

Experimental measurements were used to test an innovative approach for validating numerical models, which make use of vibration signals recorded at specific measurement points of the structure. The proposed approach involves the numerical simulation of the structural response and its comparison with the experimental one recorded at the measurement points A to F shown in Figure 9. The comparison is performed in terms of peak frequencies of power spectral density (PSD) of acceleration time–histories. In order to perform numerical analyses, the south vault of the basilica was modelled using finite element software Straus7.[25] Geometry was obtained from available geometric surveys of the basilica.

Two different models have been tested: model 1, represented in Figure 11a, representing only the vault structure; model 2, shown in Figure 11b, in which the vault and a small portion of the basilica down to the matroneum floor have been modelled. The latter model includes the south wall with the rose window, the two piers that serve as support to the north, the vault, and the internal and external curb walls present on its extrados. The two lateral wall structures were also modelled, as they provide relevant contributions to the stiffness of the system.

It is worth noting that the base level is different in the two models. Model 1 lies at the vault springer level, while the base of model 2 coincides with the matroneum floor. Both models represent only a portion of the overall structure of the basilica. This choice was adopted to limit the complexity of the models and the computational burden. Some further simplifications in the modelling were consciously adopted, particularly with regards to the constraint conditions. Base nodes were constrained in a fixed manner for both models. No constraint conditions were applied to the side surfaces of the models. So, although the vertical stiffness of the base restraints is higher than the real one, the models are under-constrained along the horizontal directions, with respect to the real constraint condition of the structure. These
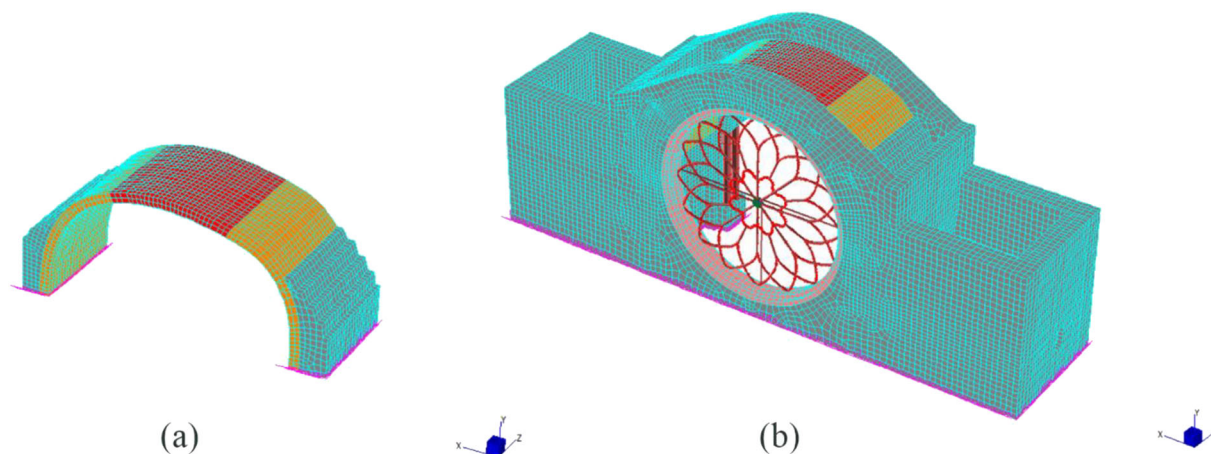


**FIGURE 11** Numerical models of the vault: (a) model 1, vault only; (b) model 2, vault with supporting structure down to matroneum floor

assumptions are partly related to the difficulty in defining precise constraint conditions, due to the high complexity of the analysed structure. Surely, by making a more detailed modelling, it is possible to obtain more accurate results in the comparison between experimental data and numerical analysis. Due to the assumed constraint conditions, the choice of the model constraint conditions will directly influence the vibration frequencies obtained from the modal analysis. It has been so necessary to take into account these uncertainties in the analysis of the results.

Material mechanical properties used for the models are shown in Table 1. They have been adopted according to literature and to sonic tests results presented in Section 3. The central portion of the vault, presenting spread cracking, was modelled using a reduced elastic modulus. Elastic modulus values for masonry walls and both undamaged and cracked portions of the vault were adopted in agreement with sonic tests results. Stone properties have been assumed according to Oñate et al.[14]

Tables 2 and 3 show the cyclic frequencies and the translational and rotational modal participation factors of the first six modes of vibration with modal participation factor greater than or equal to 5%. Modal deformations related to these modes are represented in Figures 12 and 13.

To simulate the ambient vibration response of the structure, time-history analyses with step-integration were carried out for both numerical models. In order to model the source of ambient vibrations, acceleration histories were applied at the base of the models. Structural damping was implemented using Rayleigh's approach, as described in Chopra.[26]

**TABLE 1** Material properties assumed for numerical analyses

| Elements | Material | $E$ (MPa) | $\nu$ (−) | $\rho \left(\frac{\text{kg}}{\text{m}^3}\right)$ |
| --- | --- | --- | --- | --- |
| Piers and walls | Masonry | 4000 | 0.15 | 2000 |
| Vault | Masonry | 3000 | 0.15 | 2000 |
| Vault (cracked) | Masonry | 1750 | 0.15 | 2000 |
| Columns and rose window | Stone | 60,000 | 0.15 | 2700 |

**TABLE 2** Characteristics of vibration modes for model 1

| Mode (−) | f (Hz) | PF - Trasl. (Long) (%) | PF - Trasl. (Trasv) (%) | PF - Trasl. (Vert) (%) | PF - Rot. (Long) (%) | PF - Rot. (Trasv) (%) | PF - Rot. (Vert) (%) |
| --- | --- | --- | --- | --- | --- | --- | --- |
| 1 | 8.053 | 26.966 | 1.636 | 0.000 | 0.089 | 3.727 | 18.733 |
| 2 | 10.809 | 2.151 | 7.941 | 0.000 | 0.436 | 0.297 | 1.479 |
| 3 | 12.216 | 0.000 | 0.000 | 20.145 | 31.734 | 0.012 | 0.000 |
| 4 | 18.797 | 30.344 | 0.669 | 0.000 | 0.037 | 4.205 | 24.994 |
| 5 | 22.654 | 0.000 | 0.000 | 19.869 | 22.016 | 1.267 | 0.000 |
| 6 | 27.040 | 0.000 | 5.957 | 0.000 | 0.324 | 0.000 | 0.007 |

**TABLE 3** Characteristics of vibration modes for model *2*

| Mode (−) | f (Hz) | PF - Trasl. (Long) (%) | PF - Trasl. (Trasv) (%) | PF - Trasl. (Vert) (%) | PF - Rot. (Long) (%) | PF - Rot. (Trasv) (%) | PF - Rot. (Vert) (%) |
| --- | --- | --- | --- | --- | --- | --- | --- |
| 1 | 10.184 | 0.008 | 53.699 | 0.096 | 78.441 | 0.003 | 0.446 |
| 2 | 13.049 | 21.291 | 0.045 | 0.006 | 0.210 | 10.157 | 36.784 |
| 3 | 15.853 | 34.656 | 0.003 | 0.000 | 0.034 | 18.905 | 10.169 |
| 4 | 18.253 | 0.011 | 11.599 | 1.412 | 2.238 | 0.011 | 0.005 |
| 5 | 20.304 | 0.458 | 8.539 | 0.489 | 3.851 | 0.232 | 5.166 |
| 6 | 25.537 | 9.898 | 0.083 | 0.127 | 0.017 | 1.812 | 2.318 |

| 8.053 Hz | 10.809 Hz | 12.216 Hz |

| 18.797 Hz | 22.654 Hz | 27.040 Hz |
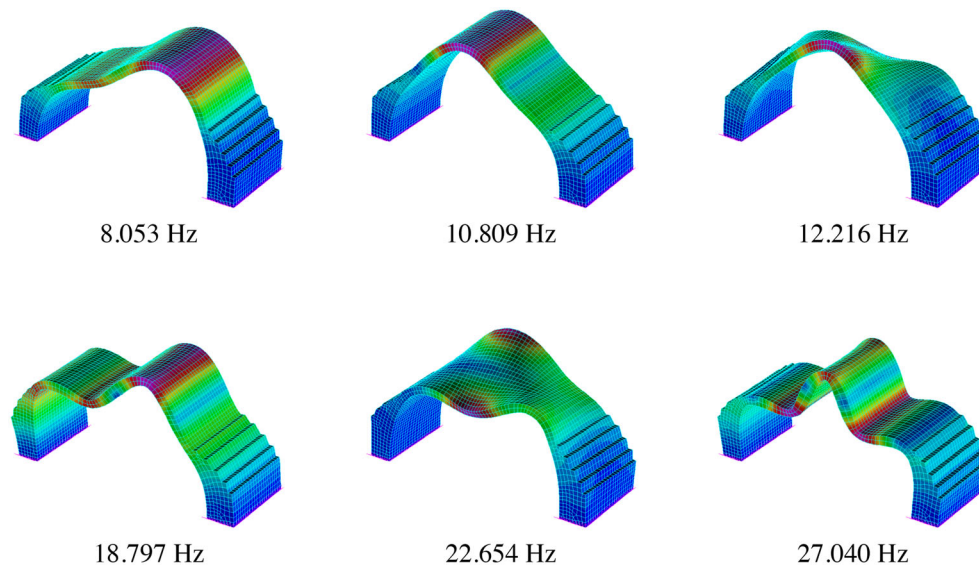
**FIGURE 12** The first six vibration modes for numerical model 1



| 10.184 Hz | 13.049 Hz | 15.853 Hz |

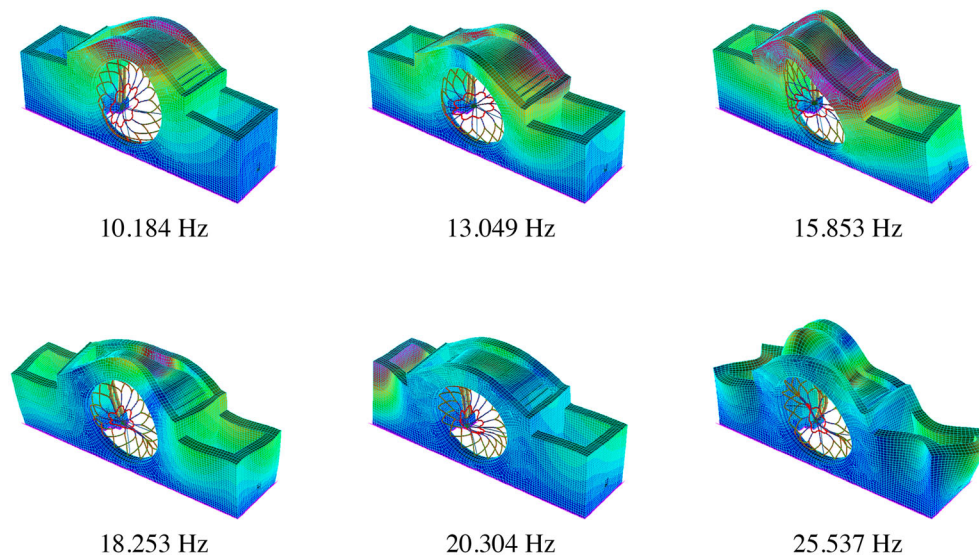| 18.253 Hz | 20.304 Hz | 25.537 Hz |

**FIGURE 13** The first six vibration modes for numerical model 2

Values of damping ratio and frequencies on which they are imposed needs to be defined carefully. Any vibration mode having a frequency which lay largely outside the chosen range is heavily damped. A damping ratio $\xi = 4\%$ was adopted, following considerations reported in Elmenshawi et al.[27] for medium-damaged masonry structures. This value has been imposed at frequencies equal to 8 Hz and 20 Hz.

Acceleration histories recorded along the three directions at the matroneum (reference point in Figure 9) were used to generate the input signals to be applied to the numerical models.

The acceleration histories recorded at 512 Hz were down-sampled at 64 Hz. The Fourier spectra of the signals presented high amplitudes in the frequency range between 0 Hz and 2.5 Hz, with an exponential increase in amplitude approaching zero frequency value, indicating an almost constant component is present in the signal. In the absence of more detailed investigations, it was impossible to clarify the source of the high amplitude values observed at low frequencies, although they could be due to an ambient noise source. Since these signals were intended to be used to simulate an ambient vibration source on the supporting structure of the vault, there was the need to eliminate constants in the history of motion. Acceleration signals were filtered using a high-pass filter, deleting the components with a frequency lower than 2.5 Hz. A 300-s-long portion was selected from every filtered component to be used as input for

numerical analyses. Figure 14a shows the time histories and Fourier spectra of the acceleration inputs obtained from the data recorded at matroneum. It can be seen that amplitudes of transverse component are larger than those of longitudinal and vertical ones.

It is worth underlining that in some cases, experimentally recorded accelerometric input may not be available. So, other kinds of signals (e.g., artificially generated white noise signals) are sometimes employed as an input source for time-history analyses.

To compare results obtained using artificially generated signals and in situ recorded ones, a set of artificial input signals was also generated to be used as input for the numerical analyses. It consists of Gaussian white noise histories with a maximum value of 0.00035 $m/s^2$, high-pass filtered to eliminate components with frequencies in the range 0–2.5 Hz, so as to make them comparable with experimentally derived inputs. The time histories and Fourier spectra of white noise input signals are presented in Figure 14b.
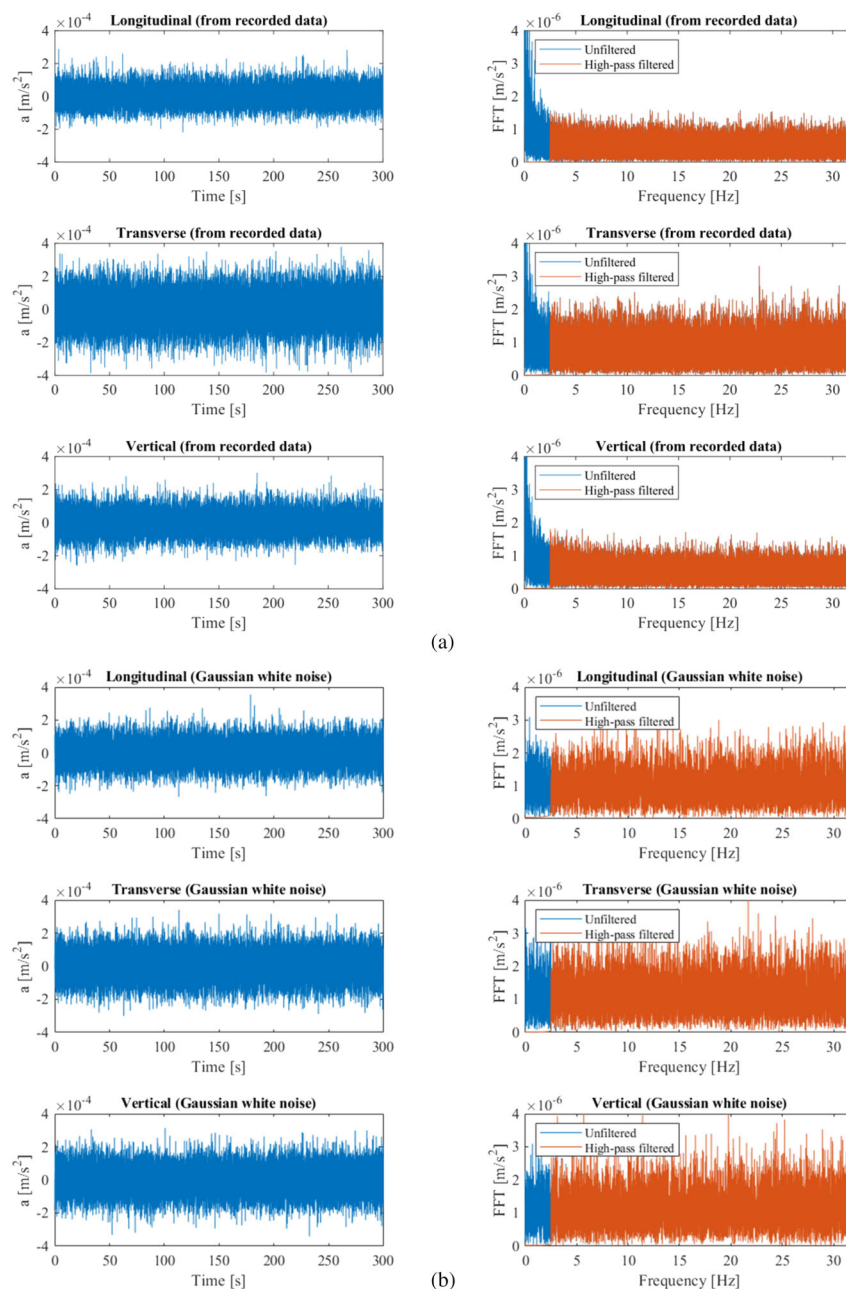


**FIGURE 14** Input acceleration signals for numerical analyses: (a) obtained from in situ recorded acceleration data at matroneum; (b) generated white Gaussian noise

Time-history analyses allowed to calculate acceleration response at the measurement points of the vault (points A to F in Figure 9). In all analyses, the structural response was not solved throughout the whole input history, because of the limited memory capacity of the software. Due to this restriction, numerical time-history responses were 180 s long and 30 s long for models 1 and 2, respectively. Power spectral density (PSD) spectra for experimental and numerical acceleration signals were evaluated using the P-Welch method. A triangular window having a length equal to 150/64 times the sampling frequency has been used. Figures 15–20 show a comparison between numerical and experimental PSD spectra for all the vault measurement points (A to F).

The spectra obtained from artificial and recorded inputs are similar in many cases. Nevertheless, significant differences have been detected for model 2 in components along the transverse direction. An indication of the dependency of spectrum shape on the type of input signal was also highlighted by Pepe et al.[12] It so appears that the choice of input signals can have a relevant impact on the frequency content of the numerical response of the structure.

Comparison between the numerical and experimental spectra can be made by comparing the respective spectrum peaks. Numerical spectra show strong amplitude components located over limited frequency ranges; that is, spectrum peaks can be quite easily identified in many cases. Conversely, experimental spectra exhibit medium-to-high amplitudes over a wide range of frequencies.

In order to clearly identify spectra peaks, normalized non-dimensional PSD spectra were created dividing spectral ordinates by the maximum PSD. The obtained spectra are presented in Figure 21, considering only numerical responses obtained using recorded inputs. Frequencies associated with maximum PSD values are also highlighted by dashed lines and summarized in Table 4, in order to provide a straightforward comparison between experimental and numerical spectra. A measure of error $\Delta f$ is introduced, defined as the percentage difference between the numerical and experimental peak frequencies. Analysing the values reported in Table 4, a quite good agreement between experimental and numerical peak frequencies can be observed for the transverse acceleration components, especially for results of numerical model 2. Good results are obtained for some cases in the comparison of vertical components, while a general poor agreement is detected regarding the spectra of longitudinal components.



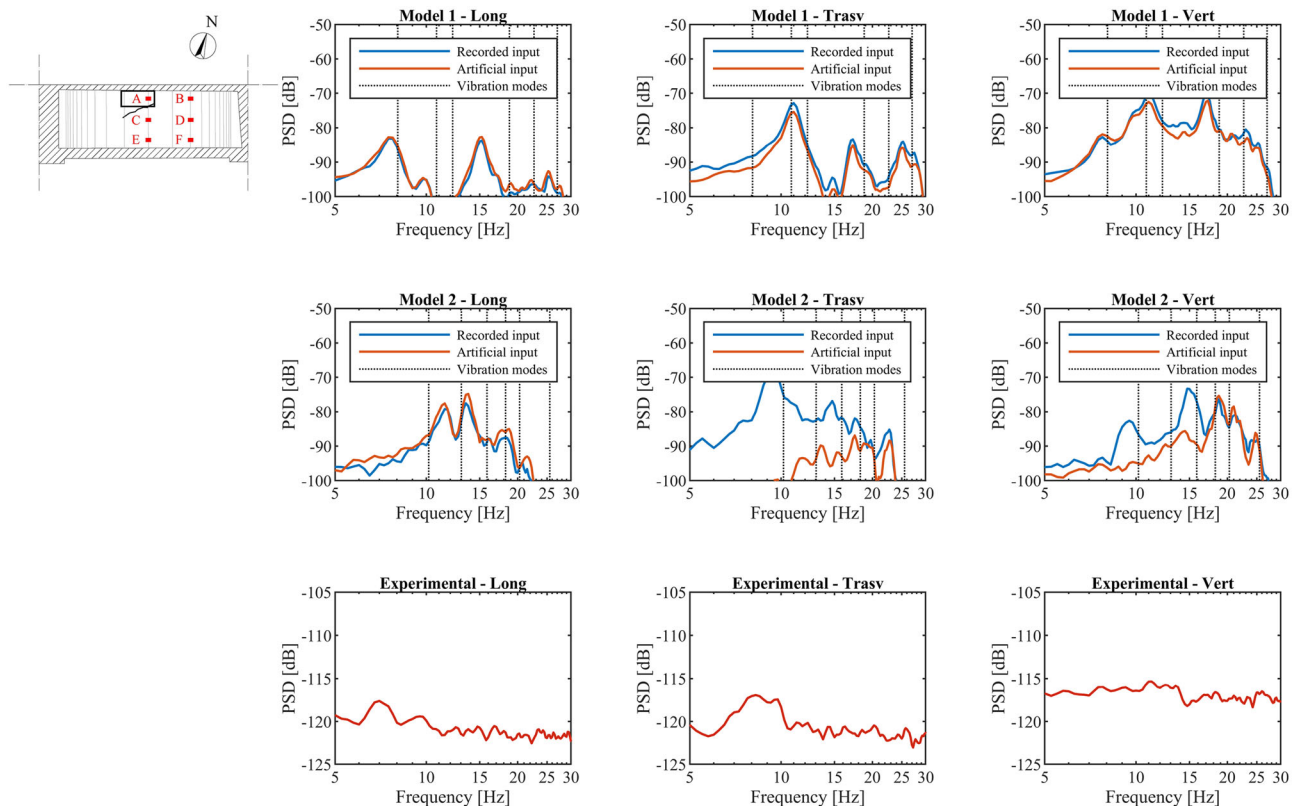**FIGURE 15** Frequency analysis of experimental and numerical acceleration histories at measurement point A
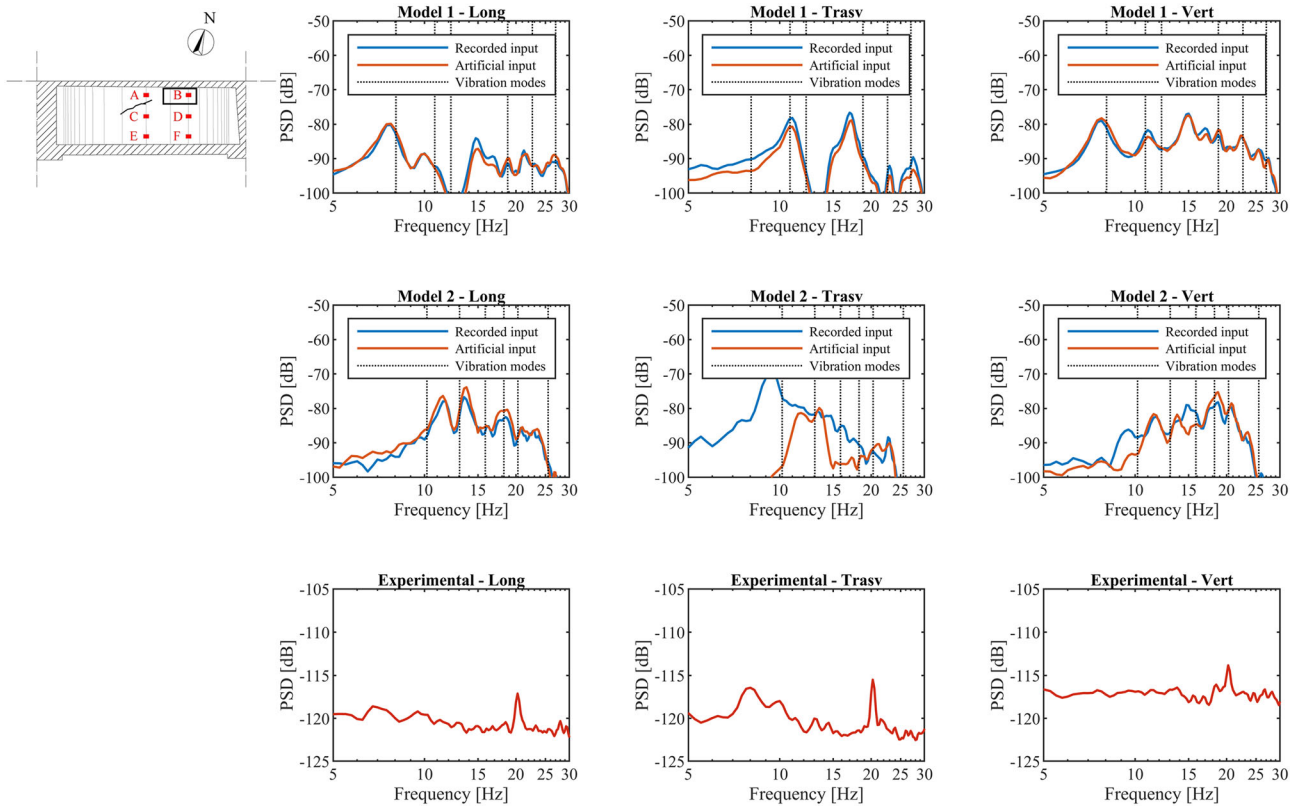
**FIGURE 16** Frequency analysis of experimental and numerical acceleration histories at measurement point B



**FIGURE 17** Frequency analysis of experimental and numerical acceleration histories at measurement point C

**FIGURE 18** Frequency analysis of experimental and numerical acceleration histories at measurement point D



**FIGURE 19** Frequency analysis of experimental and numerical acceleration histories at measurement point E

**FIGURE 20** Frequency analysis of experimental and numerical acceleration histories at measurement point F
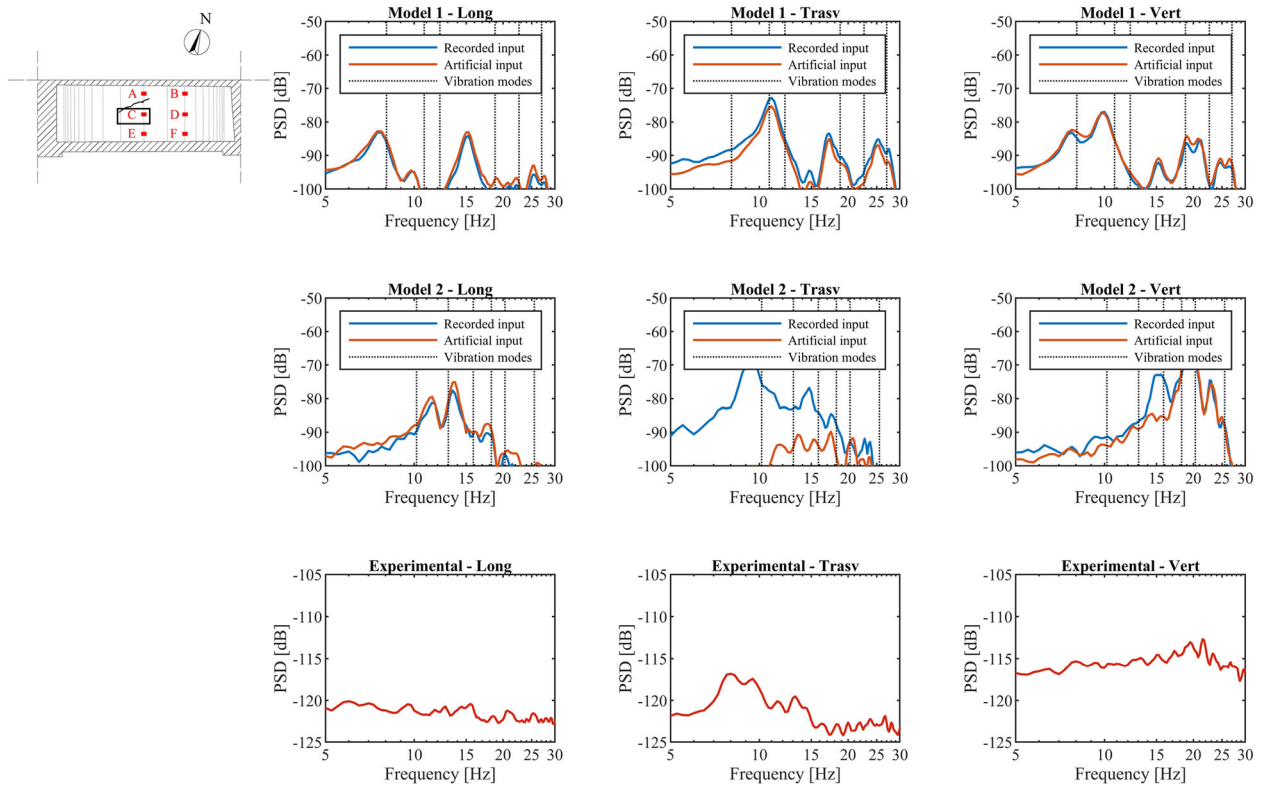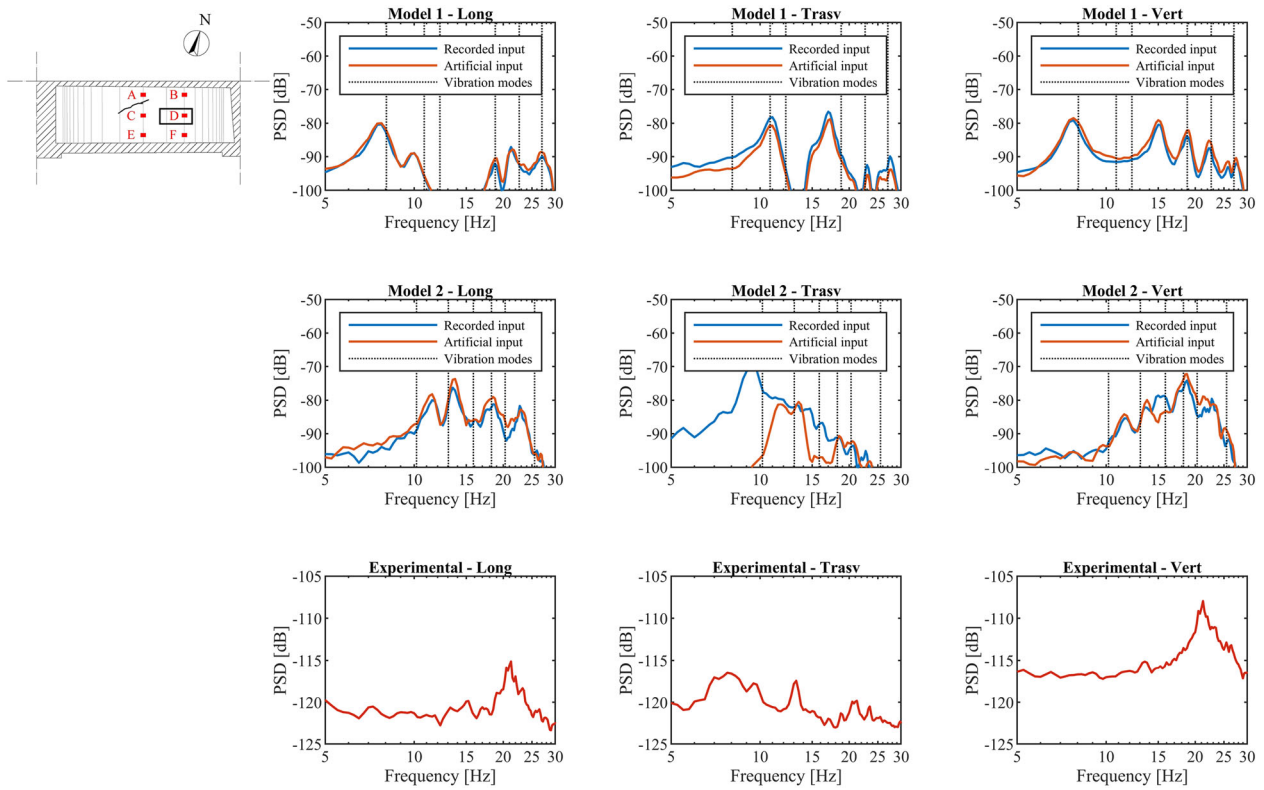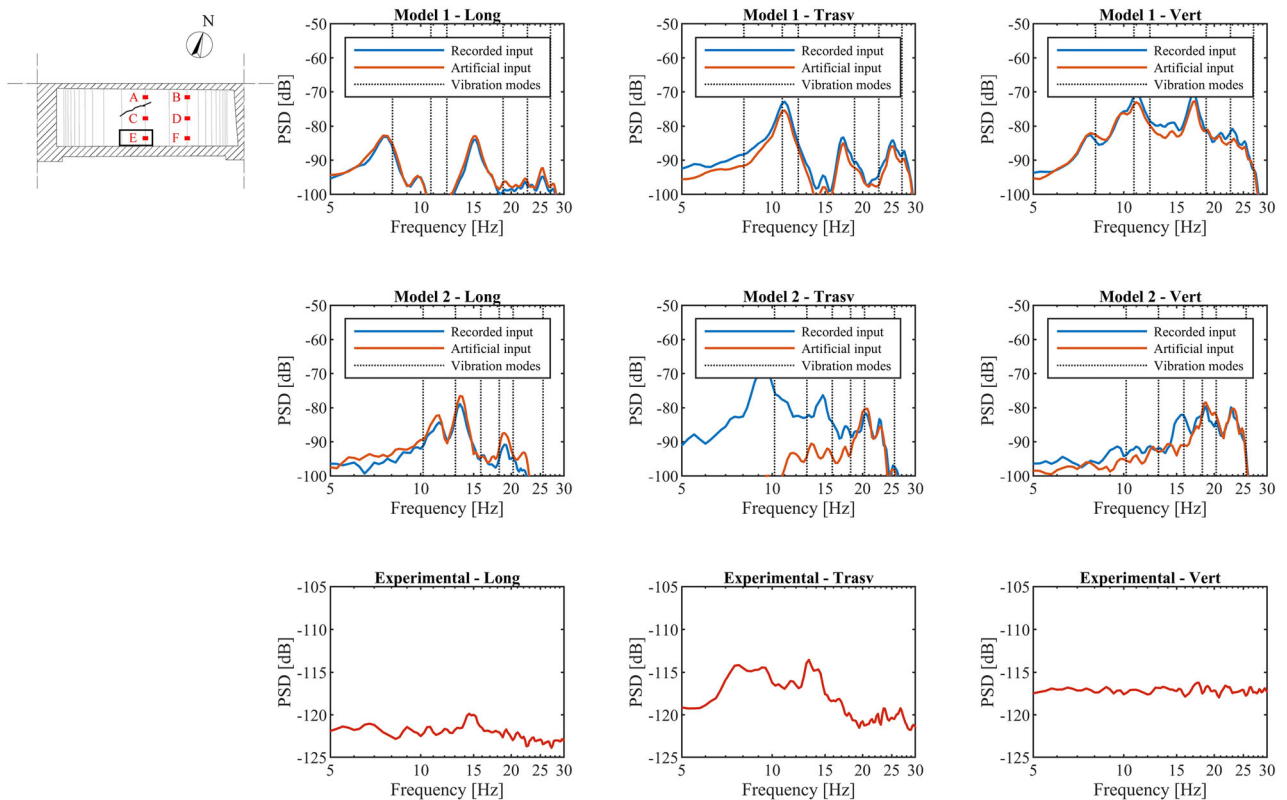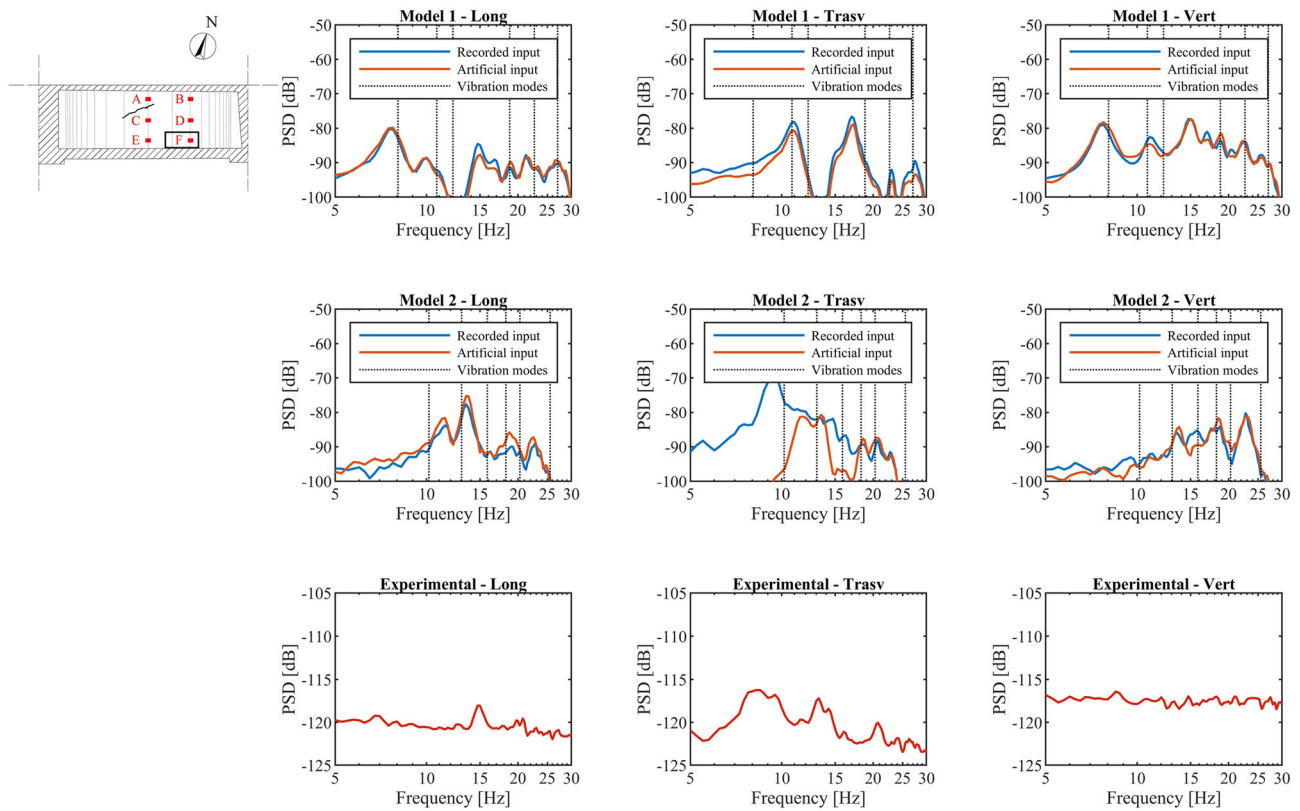
# 5 | DISCUSSION

Based on results presented in the previous sections, it is possible to formulate some hypotheses on the causes of the vault's cracking pattern, considering its boundary conditions. Stiff masonry walls vertically support the vault on the east and west sides, while the rose window offers quite stiff support on the southern side, compared with the arched structure, which supports the vault on the northern side. This constraint condition, together with the high loads resulting from the presence of the dome, may have induced cracks in the area near the central nave.

The two prominent cracks at the vault intrados and extrados are characterized by depths between 4–18 cm (intrados) and 6–16.5 cm (extrados), respectively. The diagnostic tests showed that the two cracks have a partial overlap. In that zone, the uncompromised thickness of the vault is about 1/3 of the total value. By analysing the propagation velocity distribution on the vault obtained from direct sonic tests and presented in Figure 8, the vault average propagation velocity values are found to be far below 1000 m/s. Moreover, a 28% reduction of propagation velocity is detected in the zones affected by the cracks compared with the undamaged areas. This value translates into a possible reduction of the dynamic elastic modulus up to about 44%. The presence of the cracks, therefore, induces a considerable reduction in material compactness.

Besides, the vault vibration frequencies evaluated as peak frequencies of the ambient vibration measurements FFTs are in the range 8–15 Hz, as shown in Figure 11. These values are pretty high and similar to those detected by Bovo et al.[28] for undamaged masonry arches. Therefore, it can be concluded that the vault global stiffness does not seem to be significantly affected by the reduced compactness of the material. This behaviour can be related to the particular geometry and constraint conditions of the examined vault. In fact, the lateral masonry kerbs and the vast massive structure of the supports contribute to making the vault as a whole very rigid, despite the presence of local damage and the fact that the material shows a poor state of conservation. In this sense, there seems to be a faint correlation between the propagation velocity values measured by sonic tests and modal frequency values evaluated through ambient vibration measurements for the examined vault. Such a result is proper of complex and articulated structures, which is the case of several historic masonry structures. Therefore, since for this kind of buildings a poor correlation between results
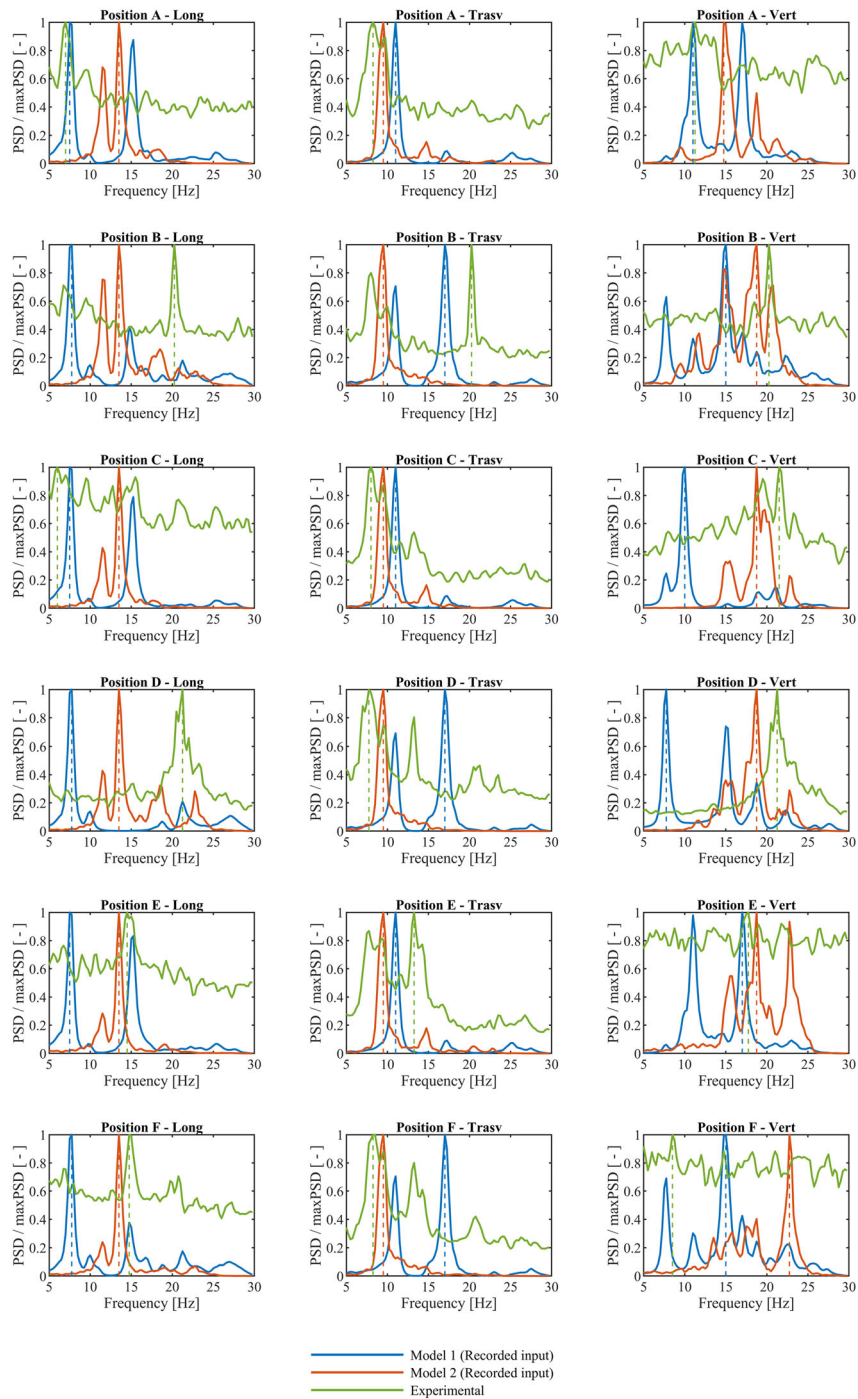
**FIGURE 21** Comparison of numerical and experimental PSD spectra normalized to their maximum value, for points A to F

of local sonic tests and global ambient vibration measurements is expected, both types of tests are fundamental to be performed in order to correctly detect the stiffness and the state of conservation of the structure.

Data from sonic and ambient vibration measurements can also be useful in validating numerical models, especially for complex heritage structures in which several uncertainties arise in the modelling phase. The proposed validation approach is based on comparing experimental and numerical peak frequencies of the structural response to ambient vibration. By applying this procedure to the studied vault, some considerations have been drawn. The best correspondence of experimental and numerical peak frequencies is observed for the spectra of transverse components, especially for positions C and D, which are located in the central zone of the vault. For these points, a good match is also found for the vertical components, with percentage differences less than 15%. It is worth noting that in several cases, the

**TABLE 4** Summary of frequencies associated to maximum PSD values

| Device position | Type of result | Longitudinal | | Transversal | | Vertical | |
|---|---|---|---|---|---|---|---|
| | | $f$ (Hz) | $\Delta f$ (%) | $f$ (Hz) | $\Delta f$ (%) | $f$ (Hz) | $\Delta f$ (%) |
| A | Numerical 1 | 7.5 | 7.14 | 11 | 33.33 | 11 | −2.22 |
| | Numerical 2 | 13.5 | 92.86 | 9.5 | 15.15 | 14.75 | 31.11 |
| | Experimental | 7 | - | 8.25 | - | 11.25 | - |
| B | Numerical 1 | 7.75 | −61.73 | 17 | −16.05 | 15 | −25.93 |
| | Numerical 2 | 13.5 | −33.33 | 9.5 | −53.09 | 18.75 | −7.41 |
| | Experimental | 20.25 | - | 20.25 | - | 20.25 | - |
| C | Numerical 1 | 7.5 | 25.00 | 11 | 37.50 | 10 | −53.49 |
| | Numerical 2 | 13.5 | 125.00 | 9.5 | 18.75 | 18.75 | −12.79 |
| | Experimental | 6 | - | 8 | - | 21.5 | - |
| D | Numerical 1 | 7.75 | −63.53 | 17 | 119.35 | 7.75 | −63.53 |
| | Numerical 2 | 13.5 | −36.47 | 9.5 | 22.58 | 18.75 | −11.76 |
| | Experimental | 21.25 | - | 7.75 | - | 21.25 | - |
| E | Numerical 1 | 7.5 | −48.28 | 11 | −16.98 | 17 | −4.23 |
| | Numerical 2 | 13.5 | −6.90 | 9.5 | −28.30 | 18.75 | 5.63 |
| | Experimental | 14.5 | - | 13.25 | - | 17.75 | - |
| F | Numerical 1 | 7.75 | −47.46 | 17 | 106.06 | 15 | 76.47 |
| | Numerical 2 | 13.5 | −8.47 | 9.5 | 15.15 | 22.75 | 167.65 |
| | Experimental | 14.75 | - | 8.25 | - | 8.5 | - |

spectra are characterized by many peaks with similar amplitudes, and by considering only the higher one, a misleading interpretation of the results can be obtained. In fact, it can be seen in Figure 21 how for the transverse component the numerical model 2 provides a quite good agreement for all points A to F. Conversely, neither model 1 nor model 2 seems capable of providing an effective and consistent representation of experimental spectra shapes for the longitudinal direction. In particular, only some peaks correspondence is observed for model 2, especially for points E and F, which are the most far from the dome.

Based on the numerical results of model 2, some considerations on the dynamic behaviour of the vault have been formulated. Analysing the modes of vibration provided by the model, high modal participations were found in the first three modes considered. In particular, the second mode, having a frequency equal to 13 Hz, presents a torsional modal form that generates a high state of stress of the vault in its plane, as illustrated by the distribution of the tangential strains presented in Figure 22. This state of stress generates a tensional distribution that tends to accentuate the pattern of cracks observed at the extrados and intrados of the vault.

It is worth to note that the partial agreement observed in some of the comparison between experimental and numerical results should be read considering the assumptions and simplifications adopted in the numerical modelling procedure. In particular, an important role is played by the fact that, due to the computational burden, only a portion of the whole structure has been modelled, with the consequent need to adopt simplified constraint conditions. Another critical aspect, which may influence the result of the proposed procedure, concerns the representation of the input in the time-history analysis, both concerning the portions of the model on which it is imposed and with regards to the input type, which may be experimentally recorded or artificially generated. However, the presented results appear highly valuable to illustrate how the proposed procedure can be implemented, highlighting its benefits and crucial aspects.

The proposed procedure can be a consistent method to validate the results provided by numerical models, and its use can be advantageous in many cases. In fact, despite traditional experimental campaigns based on operational modal analysis allow a complete reconstruction of vibration modes and modal shapes of the structure based on the measured data, they often involve high costs, which are not always sustainable. Otherwise, the proposed procedure requires to experimentally measure acceleration histories only in a limited number of selected points of the structure, providing
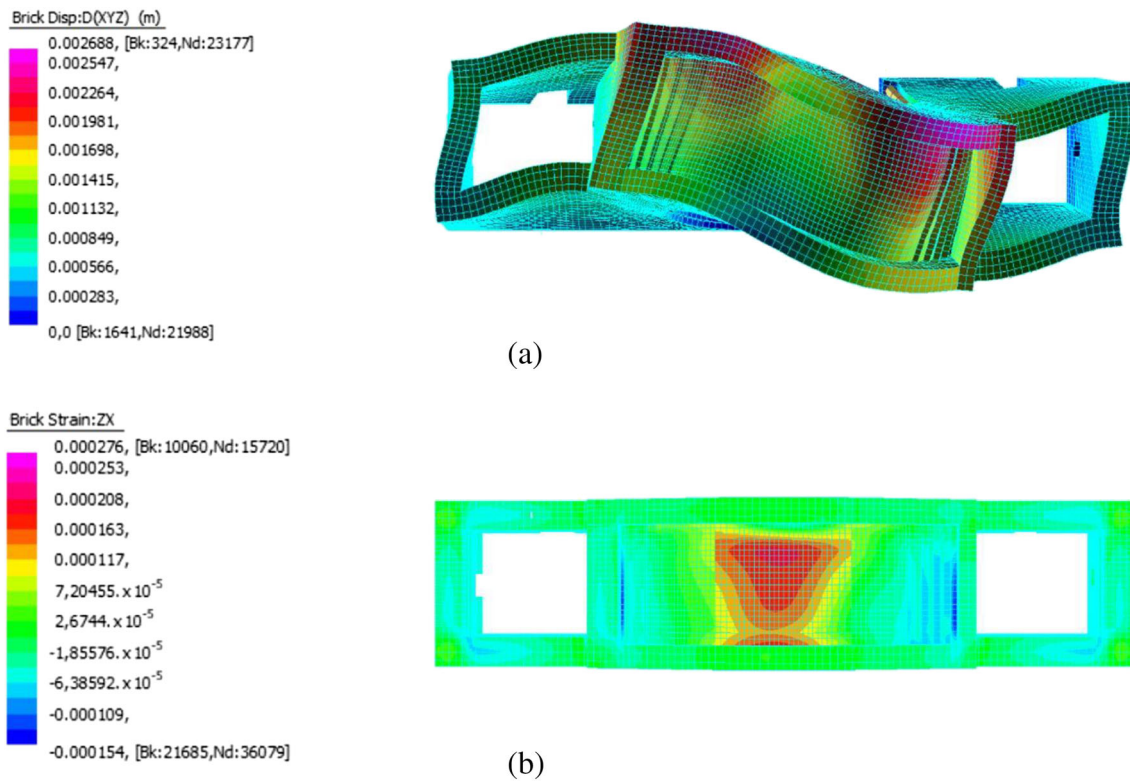
Brick Disp:D(XYZ) (m)

0.002688, [Bk:324,Nd:23177]
0.002547,
0.002264,
0.001981,
0.001698,
0.001415,
0.001132,
0.000849,
0.000566,
0.000283,
0,0 [Bk:1641,Nd:21988]

(a)

Brick Strain:ZX

0.000276, [Bk:10060,Nd:15720]
0.000253,
0.000208,
0.000163,
0.000117,
$7{,}20455. \times 10^{-5}$
$2{,}6744. \times 10^{-5}$
$-1{,}85576. \times 10^{-5}$
$-6{,}38592. \times 10^{-5}$
-0.000109,
-0.000154, [Bk:21685,Nd:36079]

(b)

**FIGURE 22** First torsional vibration mode (13.049 Hz) for numerical model 2: (a) modal deformation; (b) distribution of tangential strains on the vault. Values on the legend are normalized

helpful information for a first calibration or a final validation of a numerical model of the studied building, at a meagre cost compared to that of traditional approaches for experimental structural characterization.

## 6 | CONCLUSIONS

The presented paper investigates the benefits and crucial aspects of the combined use of sonic tests and ambient vibration measurements for the structural characterization of cultural heritage buildings. An experimental campaign carried out on the south vault of St. Mark's Basilica in Venice is presented, and the results are used both to characterize the structural behaviour and state of conservation of the vault and to illustrate a procedure for the calibration/validation of numerical models. Based on the presented experimental investigations and the performed numerical analyses, the following final considerations are proposed:

- The analysis of data obtained from the two different types of ND tests has highlighted how the interaction between local damage and global structural behaviour can be complex, especially in historic masonry buildings. In this kind of structures, the correlation between measures related to the global structural behaviour, such as ambient vibrations, and measures of local properties, such as propagation velocities, can be influenced by multiple factors. Among these, the complexity of geometry, boundary conditions and mass distribution play a prominent role. In the analysed case study, the sonic tests have provided velocity values associated with a reduced degree of compactness of the material, while the structure vibration frequencies derived from ambient vibration measurements have shown to be comparable to those of undamaged masonry structures;
- In the analysed vault, the particular support conditions together with the non-symmetrical distribution of loads and material mechanical degradation are identified as the leading causes of the formation of cracks in the zone of the vault near to the south dome of the basilica;
- The proposed numerical model validation procedure was applied to the case study vault, showing an agreement between experimental and numerical response to ambient vibration, especially evident for the acceleration

components along the transverse direction of the vault. Though further investigations are required, the proposed approach appears promising since it provides a validation test for numerical models based on a minimal number of recorded acceleration histories;

- Analysing the modes of vibration provided by the model, high modal participations were found in the first three modes considered. In particular, the second mode, having a frequency approximately equal to 13 Hz, has a torsional modal shape that generates a high state of stress in the plane of the vault, as illustrated by the associated distribution of tangential strains.

## ACKNOWLEDGEMENTS

## DATA AVAILABILITY STATEMENT

The data that support the findings of this study are available from the corresponding author upon reasonable request.

## ORCID

*Eleonora Spoldi* 🄳 https://orcid.org/0000-0002-1510-9549
*Ileana Ippolito* 🄳 https://orcid.org/0000-0003-4635-2899
*Alberto Stella* 🄳 https://orcid.org/0000-0001-9005-5248

## REFERENCES

1. Asteris PG, Chronopoulos MP, Chrysostomou CZ, et al. Seismic vulnerability assessment of historical masonry structural systems. *Eng Struct*. 2014;62–63:118-134. https://doi.org/10.1016/j.engstruct.2014.01.031

2. Lança P, Lourenço PB, Ghiassi B. Structural assessment of a masonry vault in Portugal. *Proc Inst Civ Eng: Struct Build*. 2015;168(12):915-929. https://doi.org/10.1680/stbu.14.00093

3. Betti M, Vignoli A. Numerical assessment of the static and seismic behaviour of the basilica of Santa Maria all'Impruneta (Italy). *Construct Build Mater*. 2011;25(12):4308-4324. https://doi.org/10.1016/j.conbuildmat.2010.12.028

4. Berto L, Doria A, Faccio P, Saetta A, Talledo D. Vulnerability analysis of built cultural heritage: a multidisciplinary approach for studying the Palladio's Tempietto Barbaro. *Int J Archit Heritage*. 2017;11(6):773-790. https://doi.org/10.1080/15583058.2017.1290853

5. Mola F, Vitaliani R. Analysis, diagnosis and preservation of ancient monuments: The St. Mark's Basilica in Venice. In: Roca P, Gonzalez JL, Mari AR, Onate E, eds. *Structural Analysis of Historical Construction*. Barcelona: CIMNE; 1996.

6. Rossi PP, Rossi C. Surveillance and monitoring of ancient structures: recent developments. Structural Analysis of Historical Construction II. 1998;1-15.

7. Russo S. Integrated assessment of monumental structures through ambient vibrations and ND tests: the case of Rialto Bridge. *J Cult Herit*. 2016;19:402-414. https://doi.org/10.1016/j.culher.2016.01.008

8. Binda L, Saisi A. Non destructive testing applied to historic buildings: the case of some Sicilian Churches. In Lourenço PB, Roca P, eds. *Historical Constructions 2001. Possibilities of numerical and experimental techniques*. Guimares, Portugal: University of Minho; 2001:29-34. http://www.hms.civil.uminho.pt/events/historica2001/

9. Castellaro S, Perricone L, Bartolomei M, Isani S. Dynamic characterization of the Eiffel Tower. *Eng Struct*. 2016;126:628-640. https://doi.org/10.1016/j.engstruct.2016.08.023

10. Russo S, Liberatore D, Sorrentino L. Combined ND techniques for structural assessment: the case of historic Nepali constructions after the 2015 Gorkha earthquake. *Proceedings of ICEM2018: The 18th International Conference on Experimental Mechanics*. MDPI proceedings. Vol 2. 421st ed. 2018:1-7. https://www.mdpi.com/2504-3900/2/8/421

11. Farrar CR, Park G, Allen DW, Todd MD. Sensor network paradigms for structural health monitoring. *Struct Control Health Monit*. 2006;13(1):210-225. https://doi.org/10.1002/stc.125

12. Pepe V, De Angelis A, Pecce MR. Numerical simulation of ambient vibration tests: a case study. 7AESE: 7th International Conference on Advances in Experimental Structural Engineering, Pavia, 2017.

13. Rossi PP. Analisi Delle Condizioni Statiche Della Basilica di San Marco a Venezia (in Italian) 1995: 1-23. https://www.rteknos.it/web/pubblicazioni/

14. Oñate E, Hanganu A, Barbat A, et al. Structural analysis and durability assessment of historical constructions using a finite element damage model. In: Roca P, Gonzalez JL, Mari AR, Onate E, eds. *Structural Analysis of Historical Constructions*. Barcelona: CIMNE; 1996.

15. Fregonese L, Taffurelli L, Adami A, et al. Survey and modelling for the bim of Basilica of San Marco in Venice. *Int Arch Photogramm Remote Sens Spat Inf Sci - ISPRS Arch*. 2017;XLII(2/W3):303-310. https://www.int-arch-photogramm-remote-sens-spatial-inf-sci.net/XLII-2-W3/303/2017/

16. Vio E. *La basilica di San Marco da cappella ducale a cattedrale della città: storia, procuratori, proti e restauri (in Italian)*. Milano: Springer; 2011 DOI: 10.1007/978-88-470-1854-9_2.

17. Beskhyroun S, Wegner LD, Sparling BF. New methodology for the application of vibration-based damage detection techniques. *Struct Control Health Monit*. 2012;19(8):632-649. https://onlinelibrary.wiley.com/doi/abs/10.1002/stc.456

18. Berra M, Binda L, Anti L, Fatticcioni A. Utilization of sonic tests to evaluate damaged and repaired masonries. Nondestructive Evaluation of Civil Structures and Materials Federal Highway Administration; and National Science Foundation., 1992.

19. Livingston RA. Nondestructive testing of historic structures. *Archiv Museum Inform*. 1999;13(3–4):249-271. https://doi.org/10.1023/A:1012416309607

20. Binda L, Saisi A, Tiraboschi C. Application of sonic tests to the diagnosis of damaged and repaired structures. *NDT E Int*. 2001;34(2):123-138. https://doi.org/10.1016/S0963-8695(00)00037-2

21. MOHO s.r.l. Tromino https://moho.world/tromino/ [accessed April 15, 2021].

22. MOHO. Software Grilla® (in Italian). 2021. http://www.tromino.it/Italiano/frameset-grilla.htm

23. MathWorks. Matlab R2021a. 2021. https://mathworks.com/products/matlab.html

24. Russo S, Spoldi E. Dynamic characterization of Nepali masonry temples hit by 2015 earthquake. *Key Eng Mater*. 2019;817:659-664. https://doi.org/10.4028/www.scientific.net/KEM.817.659

25. Straus 7. http://www.straus7.com/ [accessed April 15, 2021].

26. Chopra AK. *Dynamics of Structures*. Pearson; 2017. https://www.pearson.com/us/higher-education/program/Chopra-Dynamics-of-Structures-5th-Edition/PGM1101746.html

27. Elmenshawi A, Sorour M, Mufti A, Jaeger LG, Shrive N. Damping mechanisms and damping ratios in vibrating unreinforced stone masonry. *Eng Struct*. 2010;32(10):3269-3278. https://doi.org/10.1016/j.engstruct.2010.06.016

28. Bovo M, Mazzotti C, Savoia M. Structural behaviour of historical stone arches and vaults: experimental tests and numerical analyses. *Key Eng Mater*. 2014;628:43-48. https://doi.org/10.4028/www.scientific.net/KEM.628.43